HHS Public Access

Author manuscript

Phytomedicine. Author manuscript; available in PMC 2025 December 01.

Published in final edited form as:

Phytomedicine. 2024 December ; 135: 156086. doi:10.1016/j.phymed.2024.156086.

The anticancer effects of Aronia berry extract are mediated by Chk1 and p53 in colorectal cancer

Yoh Asahi[1,2], **Caiming Xu**[1,3], **Keisuke Okuno**[1,4], **Akinobu Taketomi**[2], **Ajay Goel**[1,5]

[1]Department of Molecular Diagnostics and Experimental Therapeutics, Beckman Research Institute of City of Hope, Biomedical Research Center, Monrovia, California, USA

[2]Department of Gastroenterological Surgery I, Hokkaido University Graduate School of Medicine, Sapporo, Hokkaido, Japan

[3]Department of General Surgery, The First Affiliated Hospital of Dalian Medical University, Dalian, China

[4]Department of Gastrointestinal Surgery, Tokyo Medical and Dental University, Tokyo, Japan

[5]City of Hope Comprehensive Cancer Center, Duarte, California, USA

Abstract

Background: Aronia berry extracts (ABE) have recently been reported to possess significant anti-cancer effects in various malignancies, including colorectal cancer (CRC), due to their high polyphenolic content. However, the molecular mechanism(s) underlying the anti-cancer effects of ABE in CRC remain unclear, which is important to consider when considering their use as complementary medicine approaches in cancer.

Methods: We performed genome-wide transcriptomic profiling and pathway enrichment analysis to identify specific growth signaling pathways associated with ABE treatment in CRC cells. In addition, a series of systematic and comprehensive cell culture studies were performed to investigate the anticancer effects of ABE in SW480 and HCT116 CRC cell lines. Subsequently, these findings were validated in patient-derived 3D organoids (PDOs) models.

Results: Transcriptomic profiling analysis identified p53 signaling as one of the key enriched pathways mediating the anti-cancer activity of ABE. Analysis of public datasets revealed that Chk1, a key regulator of p53, was one of the critical targets of ABE in CRC. Chk1 and p53 activation was shown to be downregulated with ABE treatment, leading to the induction of cell

Corresponding author: Prof. Ajay Goel, Department of Molecular Diagnostics and Experimental Therapeutics, Beckman Research Institute of City of Hope, 1218 S. Fifth Avenue, Suite 2226, Biomedical Research Center, Monrovia, California 91016; ajgoel@coh.org.

AUTHOR CONTRIBUTIONS

YA, CX, KO, and AG conceived and designed the experiments. YA performed the experiments, and YA and CX analyzed the data. YA, CX, and AG wrote the manuscript. All data were generated in-house, and no paper mill was used. All authors agree to be accountable for all aspects of work, ensuring integrity and accuracy.

Declaration of competing interests/Conflict of interest: None of the authors have any conflicts to disclose.

cycle arrest (p = 0.003 – 0.014) and enhanced DNA damage (p = 0.015 – 0.026). Furthermore, these findings were validated in PDOs, where the ABE treatment resulted in significantly fewer and smaller PDOs in a concentration-dependent manner (p = 0.045 - <0.001).

Conclusions: We firstly provide evidence for the role of the p53 signaling pathway as a mediator of the anti-cancer activity of ABE, which provides a rationale for its use as a safe and effective integrative medicine approach in CRC.

Graphical Abstract

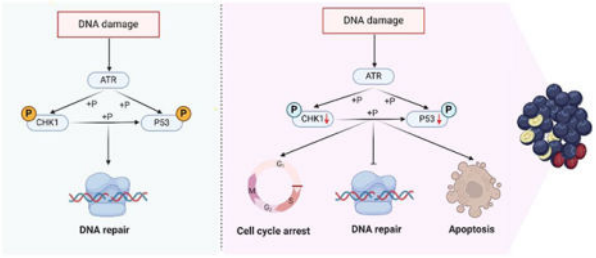

Keywords

Aronia berry; Chokeberry; colorectal cancer; p53 signaling pathway; Chk1

INTRODUCTION

Colorectal cancer (CRC) remains a major cause of cancer-related deaths worldwide, ranking second after lung cancers, with an estimated 104,270 new cases and 52,980 deaths in 2021 (Siegel et al., 2021; Sung et al., 2021). The leading cause of mortality in CRC patients is the diagnosis of the disease at an advanced stage with metastasis when curative surgery is not always possible. Systemic cytotoxic therapies are often offered to CRC patients who are not candidates for surgery. Although there have been advances in improving therapeutic regimens for the management of CRC, the overall efficacy of such treatments is significantly hampered due to the acquisition of drug resistance, toxicity, and excessive costs. More recently, many diet-based natural compounds have gained increasing research interest as complementary and alternative medicine approaches due to their overall safety, cost-effectiveness, and synergism with conventional therapies in various cancers, including CRC (Goel and Aggarwal, 2010; Goel et al., 2008b; Okuno et al., 2022). From a biological standpoint, such natural compounds are frequently enriched with abundant polyphenols that possess potent anti-inflammatory and antioxidant properties, with the ability to directly or indirectly influence multiple growth signaling pathways, making them attractive adjunct anti-cancer agents by virtue of their effects on multiple signaling pathways (Goel et al., 2008b; Okuno et al., 2022).

Among such natural compounds, interest in various berry fruits as integrative and complementary therapies has emerged due to their richness in a diverse spectrum of polyphenols and their ability to synergistically enhance the treatment efficacy in various malignancies, including CRC (Pan et al., 2015; Wang et al., 2011; Wang et al., 2013). The Aronia berries (*Aronia melanocarpa*), also known as the black chokeberries, are small,

dark, cherry-like berries native to North America. Aronia berries possess antioxidant, anti-inflammatory, and anti-bacterial properties, making them beneficial in the management of various diseases. In fact, Aronia berries are also one such berry fruit that has shown promising anti-cancer activity in several cancers. Considering that the overall polyphenolic content differs according to the species of the berries (Del Rio et al., 2010), their efficacy consequently varies in each malignancy (Bouyahya et al., 2022). For instance, Aronia berry extract (ABE) has shown significantly more potent anti-cancer effects compared to bilberry and grape seed extracts through growth inhibition in HT-29 colon cancer cells (Zhao et al., 2004). Moreover, Gao and colleagues recently revealed that ABE exerts a superior antioxidant effect in HepG2 human liver cancer cells compared to extracts from blueberry and haskap berries (Gao et al., 2018). Similarly, other studies have demonstrated the ability of Aronia berry juice to cause cell cycle arrest in human colon cancer HT-29 and Caco-2 cells (Bermudez-Soto et al., 2007). Furthermore, ABE was found to inhibit cell proliferation and increase the generation of reactive oxygen species (ROS) in HeLa, human cervical cancer cells (Rugina et al., 2012), suggesting that their antioxidant activity might be another potent mechanism for their anti-cancer efficacy. Despite the recently growing body of literature regarding their potential anti-cancer effects, the molecular mechanism(s) of the ABE in CRC remain largely unexplored. Therefore, investigating molecular underpinnings of ABE's anti-cancer activity is important to understand better its potential targets, which will allow for a more tangible rationale for its use as an integrative medicine approach in patients with CRC and potentially other malignancies.

In this study, we performed a comprehensive and systematic series of functional experiments, including cell viability, colony formation, migration, cell invasion, oxidative stress, and apoptosis assays in CRC cell lines, followed by validation of these findings in patient-derived 3D organoids (PDOs) to evaluate the anti-cancer effects of ABE. Furthermore, we undertook genome-wide transcriptomic profiling and gene set enrichment analysis to determine associations between the p53 signaling pathway and the anti-cancer effects of ABE. These investigations led us to determine that chk1 and p53 pathways play an important role in mediating the anti-cancer effects of ABE in colorectal cancer.

MATERIALS AND METHODS

Cell culture and reagents

Human CRC cell lines (SW480 and HCT116) were obtained from the American Type Culture Collection (ATCC; Manassas, VA, USA). CRC cell lines were maintained in Dulbecco's Modified Eagle's Medium (DMEM; Gibco, Carlsbad, CA) supplemented with 10% fetal bovine serum (FBS; Gibco) and 1% penicillin-streptomycin (Sigma Aldrich, St. Louis, MO, USA) in the incubator at 37°Cand 5% CO2 humidity. To harvest the adherent cells, 0.05% trypsin-0.03% EDTA (Invitrogen, Carlsbad, CA, USA) was used. Cell culture media was replenished every two to three days.

A stock solution of Aronia berry extract (ABE; generously provided by EuroPharma USA, Green Bay, WI) was dissolved in dimethyl sulfoxide (DMSO; Sigma Aldrich) at a concentration of 5 mg/mL, then kept frozen at −20°C and subsequently used for all experiments.

Cell viability

To quantify the cell viability of CRC cell lines, 5×10^3 cells per well were seeded in 96-well flat plates and incubated for 18 hours to allow adherence of the cell lines to the plate surface. After that, cells were treated with different concentrations of ABE. After 48 hours of treatment with ABE, 20 µl of MTT solution (5 mg/ml, Sigma Aldrich) was added to each well and incubated for an additional 2 hours, and thereafter, the medium was discarded. After washing the cell lines with phosphate-buffered saline (PBS), 200 µl of DMSO was added to each well and pipetted until the cell lines were fully lysed. The absorbance values for each well were measured at an optical density (OD) of 435 nm using a microplate reader (Tecan Trading AG, Männedorf, Switzerland).

Migration assay

CRC cell lines were cultured in 6-well culture plates for migration assays and observed till 90% confluence. A 'wound' was created with a sterile 200 µl micropipette tip by making a scratch in the cell monolayer. The scratched cells were removed by washing with PBS. Cells were then treated with different concentrations of ABE. Images of the cultured CRC cell lines were captured at 0 and 24 hours using an Olympus inverted microscope (magnification ×40), and the results were analyzed with Image-J 1.53s software (http://imagej.nih.gov/ij/index.html) to calculate wound closure percentages. All experiments were performed in triplicate, and representative images were provided.

Colony formation assay

Colony formation assays were conducted on CRC cell lines treated with different concentrations of ABE (IC_{25} and IC_{50}) for 48 hours. For these assays, 5×10^2 pre-treated cells per well were incubated with different concentrations of ABE in 6-well plates for 1 week. Cells were fixed to cell culture plates using 100% methanol for 30 minutes and stained with 1% crystal violet overnight. Colony areas were calculated using the Image-J 1.53s software.

Cell invasion assay

Cell invasion assays were performed in CRC cell lines treated with different concentrations of ABE (IC_{25} and IC_{50}) for 48 hours. Herein, 1.0×10^5 pre-treated cells per well were seeded into the Matrigel invasion chamber (Corning, Tehama County, CA) with an 8.0 µm PET Membrane. After 48 hours of incubation, invaded cells were fixed and stained by the Diff-Quick staining procedure. Images of the cell lines were captured with an Olympus inverted microscope (magnification ×40) to measure cell count.

Oxidative stress and Apoptosis assay

Oxidative stress and apoptosis assays in CRC cell lines were performed following 24 hours of treatment with ABE. Oxidative stress and cellular apoptosis levels were investigated using the Muse Cell Analyzer (Millipore Corp, Billerica, MA) with Oxidative Stress Kit and Annexin V & Dead Cell Kit, following the manufacturer's instructions.

RNA extraction, Genome-wide transcriptomic profiling, and gene set enrichment analysis

RNA-sequencing (RNA-seq) was performed as previously reported (Roy et al., 2022). After 24 hours of treatment with inhibitory concentration 25 (IC_{25}) concentrations of ABE or DMSO, total RNA was extracted from each cell line using miRNeasy kit (Qiagen, Hilden, Germany). Next-generation sequencing (NGS) library construction was performed on the extracted RNA with a SureSelect XT HS2 mRNA Library Preparation Kit (Agilent, Santa Clara, CA, USA) with up to 1 μg of total RNA input, following the manufacturer's instructions. Ribosomal RNA-depleted libraries were generated using 1 μg of RNA from each sample with the TruSeq RNA Sample Prep Kit (Illumina, San Diego, CA, USA). Library product size distributions and concentrations were determined using a Bioanalyzer DNA High Sensitivity Kit (Agilent Technologies, Santa Clara, CA, USA) and verified by paired sequencing (150 bp at each end). The HiSeq X-TEN system (Illumina, San Diego, CA, USA) was used for the analysis. All procedures for RNA-seq were performed in duplicate.

For the analysis of RNA-seq, FastQ files were trimmed using Trim Galore to remove the adapter sequence and 3′ bases with quality scores lower than 30 before alignment. The trimmed reads were mapped to human genome version GRCH38 and downloaded using STAR to generate alignment files. The edgeR software package was used to analyze the differentially regulated genes. Upregulated and downregulated genes were selected by a threshold of P value < 0.05 and $|\log_2 \text{Foldchange}|$ ($|\log_2 FC|$) > 0.5. The common differentially regulated genes between the two cell lines were used for Gene Ontology (GO) and Kyoto Encyclopedia of Genes and Genomes (KEGG) gene set enrichment analysis through the DAVID online tool (https://david.ncifcrf.gov/summary.jsp) [25] for determining the most relevant signaling pathways influenced by ABE in CRC cells. Package "ggplot2" was used for the pathway visualization in R.

Real-time quantitative reverse transcription PCR (RT-qPCR) assays

Total RNA was extracted from CRC cell lines after treatment with various concentrations of ABE for 24 hours. RNA was reverse transcribed to complementary DNA (cDNA) using a high-capacity Reverse Transcription Kit (Thermo Fischer Scientific, Waltham, MA). qRT-PCR assays were performed with a SensiFAST SYBR Lo-ROX Kit (Bioline, London, United Kingdom) and the QuantStudio 6/7 Flex RT-PCR System (Applied Biosystems, Foster City, CA). The primers used in the present study are depicted in Supplementary Table S1. Delta Ct values were used to calculate gene expression level differences with β-catenin as the housekeeping gene.

Protein extraction and western immunoblotting

Primary antibodies against β-actin (1:1000, #58169; Cell Signaling Technology, Danvers, MA, USA), p-Chk1 (1:1000, #2348; Cell Signaling Technology), Chk1 (1:1000, #60277–1-Ig; Proteintech, Chicago, IL, USA), p-p53 (1:1000, #9286; Cell Signaling Technology), and p53 (1:1000, #sc-126; Santa Cruz, CA, USA) and secondary antibodies (#7074 or #7076; Cell Signaling Technology) were used for western immunoblotting assays. RIPA Lysis and Extraction Buffer containing a protease inhibitor cocktail (Thermo Fischer Scientific) was used for total protein extraction from CRC cell lines after 24 hours of treatment

with different concentrations of ABE. Proteins were separated on a 10% Mini-PROTEAN TGX™ Precast Gel (BIO-RAD, Hercules, CA, USA) and transferred onto nitrocellulose membranes. The membranes were blocked with 5% bovine serum albumin (Sigma-Aldrich) in Tris buffer saline (Bio-Rad, Hercules, CA, USA) with 0.1% Tween-20 (Sigma-Aldrich) for one hour at room temperature (RT) and then incubated at 4 °C overnight with the primary antibody (1:1000). After washing 3 times with 0.1% TBST, membranes were incubated at room temperature with a secondary antibody (1:2000) for 1 hour. Immunoblots were visualized using an HRP-based chemiluminescence kit (Thermo Fisher Scientific) using the ChemiDoc-MP Imaging system (ver 5.2.1, Bio-Rad). β-actin was used as an internal control, and the relative protein levels were quantified with the Image-J 1.53s software.

DNA damage and cell cycle assays

DNA damage assays in CRC cell lines were performed by immunofluorescence and flow cytometry following the treatment with ABE for 48 hours. For the immunofluorescence assay, 5×10^5 cells per well were seeded in 6 cm flat plates with a slide in each well. After incubation for 18 hours, cells were treated with different concentrations of ABE. Cells were fixed with 4% paraformaldehyde and permeabilized in 0.5% Triton X-100. PBS containing 5% goat serum was used for blocking, and cells were incubated with a primary antibody p-H2AX (1:1000, #05–636; Proteintech, Temecula, CA, USA) overnight, followed by three washes with 0.1 % PBST. Cells were incubated for 1 hour with fluorescent-conjugated secondary antibodies (1:1000 dilution), followed by three washes, and cell nuclei were stained. Cells were imaged using a fluorescent microscope with 488 nm excitation and 496 nm emission in a microplate reader (Tecan Trading AG) under 160x magnification.

Cell Cycle Kit and H2A.X Activation Dual Detection Kit were used for flow cytometry analysis with Muse Cell Analyzer (Millipore Corp), following the manufacturer's instructions.

Analysis of gene expression datasets

This study included an analysis of 679 CRC cases from three publicly available gene expression datasets: The Cancer Genome Atlas (TCGA; n = 327), GSE104645 (n = 181), and GSE159216 (n = 171). TCGA data was downloaded from the University of California Santa Cruz Xena Browser (https://xenabrowser.net/). The GSE104645 and GSE159216 datasets were downloaded from the Gene Expression Omnibus database (https://www.ncbi.nlm.nih.gov/geo/).

Patient-derived 3D tumor organoids (PDOs)

Three-dimensional (3D) organoids from CRC patients were generated per the previous report (Okuno et al., 2022; Ravindranathan et al., 2018; Sharma et al., 2020; Zhao et al., 2022a; Zhao et al., 2022b). Patients were anonymously coded in compliance with the Declaration of Helsinki. A written informed consent was obtained from patients, and all experiments were approved by the Institutional Review Board of City of Hope. PDOs were seeded in a 24-well plate by forming a dome in 40 μl of Matrigel (Corning, Tehama County, CA, USA) with IntestiCult™ Organoid Growth Medium (#06010, STEMCELL

Technologies) containing epidermal growth factor (STEMCELL Technologies). 750μl of IntestiCult™ Organoid Growth Medium was added around the dome. The PDOs were treated with different concentrations of ABE for 48 hours. PDOs larger than 100 μm in size were observed, and the number and the size of PDOs were calculated with the Image-J 1.53s software.

Statistical analysis

All data are represented as mean ± standard deviation (SD). The Shapiro–Wilk test was used to test the normality of the data. The two-sided Student's t-test was performed using the software JMP (JMP Pro, version 16; SAS Institute Inc., Cary, NC) for statistical analysis to compare differences between continuous values of different groups. P-values were adjusted with Holm's method for comparing 3 groups. $P < 0.05$ was considered statistically significant.

RESULTS

ABE exhibited anti-tumor effects in CRC cells via inhibition of cell proliferation, migration, clonogenicity, and invasion.

The primary objective of our study was to examine the anti-tumor effects of ABE in CRC cell lines. We performed experiments using 2 different CRC cell lines, SW480 (microsatellite stable) and HCT116 (microsatellite unstable). MTT assays were first performed to examine the effect of ABE on the cell viability of CRC cell lines, and dose-dependent anti-proliferative effects of ABE were observed, indicating growth suppression and inhibition of cell viability in both CRC cell lines. The quarter- and half-maximal inhibitory concentrations (IC_{25} and IC_{50}) were 80.0 μg/mL and 130.0 μg/mL for SW480 and 80.0 μg/mL and 140.0 μg/mL for HCT116 cells (Fig. 1A). Accordingly, all subsequent experiments were performed using 80.0 μg/mL and 140.0 μg/mL for IC_{25} and IC_{50} concentrations.

Next, we performed migration assays to evaluate the anti-migratory effects of ABE in both CRC cells. The migration rate of CRC cells was significantly suppressed with ABE treatment at IC_{50} concentrations compared to controls, from 57% to 7% in SW480 cells ($p < 0.01$) and 61% to 11% in HCT116 cell line ($p < 0.05$; Fig. 1B). The colony formation assays were also performed, and the results revealed that ABE significantly inhibited clonogenicity of CRC cells in a dose-dependent manner ($p < 0.01$ for IC_{25} vs. IC_{50}). Compared to the control group with a 30% colony area, ABE decreased the overall colony area to 20% with IC_{25} concentrations ($p < 0.01$) and to only 5% with IC_{50} concentrations ($p < 0.001$) in SW480 cells. Similarly, in HCT116, ABE reduced the total colony area from 22% to 14% with IC_{25} doses ($p < 0.001$) and to 8% with IC_{50} concentrations ($p < 0.001$; Fig. 1C). Finally, the anti-invasive effects of ABE were also interrogated by cellular invasion assays. The relative invasion rates using IC_{25} and IC_{50} doses were 42% and 28% in SW480 ($p < 0.05 – 0.01$) and 37% and 14% in HCT116 cells ($p < 0.001$), which was yet again a dose-dependent change in these CRC cell lines ($p < 0.001$ for IC_{25} vs. IC_{50}, Fig. 1D). Altogether, our data suggests ABE possesses high potential as an anti-cancer agent in CRC cells with diverse genomic backgrounds.

ABE-induced reactive oxygen species (ROS) accumulation and enhanced apoptosis in CRC cells.

To further understand the underlying mechanism(s) for the anti-cancer effects of ABE in CRC cells, we examined its impact on the accumulation of reactive oxygen species (ROS) using an Oxidative Stress Kit. We analyzed the results with a Muse Cell Analyzer. In SW480 cells, ABE treatment with an IC_{50} dose significantly enhanced ROS accumulation in the CRC cells to 21% compared with 6% in the control group ($p < 0.05$). Similarly, in HCT116 cells, both IC_{25} and IC_{50} concentrations significantly increased ROS accumulation in the CRC cells to 36% compared with 11% in the control group ($p < 0.05$; Fig. 2A).

Next, Annexin V binding assays were performed to evaluate the impact of ABE on apoptotic rates in CRC cell lines. ABE significantly induced apoptosis in both SW480 and HCT116. For SW480, the apoptosis induction rate was significantly increased to 22% with the IC_{50} concentrations vs. the 7% in the control group ($p < 0.05$). Likewise, in HCT116 cells, the apoptosis rate was significantly increased to 32% with the IC_{25} dose ($p < 0.01$) and to 39% at the IC_{50} concentrations ($p < 0.01$), compared to 10% in the control group (Fig. 2B). Collectively, our data demonstrated that ABE's anti-cancer effect was related to ROS accumulation and increased cellular apoptosis in CRC cells.

Transcriptomic analysis revealed an association of the p53 signaling pathway following ABE treatment in CRC cells.

To identify the molecular pathways associated with the anti-cancer effects of ABE in CRC cells, we performed a comprehensive genome-wide transcriptomic analysis using RNA-seq in ABE-treated and untreated SW480 and HCT116 cell lines. By comparing the ABE treatment group with the control group, upregulated and downregulated genes were extracted based on $|\log_2 FC| > 0.5$ and $P < 0.05$ in each cell line. Four hundred thirty-nine common differentially regulated genes in both cell lines were detected, which was defined as an aggregate of common upregulated and downregulated genes (Fig. 3A). GO and KEGG enrichment pathway analyses of these differentially regulated genes were performed, and the p53 signaling pathway emerged as the most prominent among the top 10 enriched KEGG pathways (Fig. 3B) with 8 common differentially regulated genes (Fig. 3C). More importantly, it was particularly interesting, given that the p53 signaling pathway plays a crucial role in the progression of various malignancies including CRC, rendering it a prominent target for systemic therapies (Hernandez Borrero and El-Deiry, 2021). Subsequent qRT-PCR assays of the p53-pathway-related genes confirmed that almost half of these differentially regulated genes, including ATR, CCNB1, SESN2, and SFN, were consistent with the result of a genome-wide transcriptomic analysis with statistical significance ($p < 0.05 – 0.001$; Fig. 3D). Collectively, the p53 signaling pathway was identified as a candidate pathway associated with the mechanism of anti-cancer efficacy of ABE in CRC cells.

ABE inhibited Chk1 phosphorylation in CRC cells.

Checkpoint kinase 1 (Chk1) is a key regulator that modulates p53 in cancers that exert an anti-cancerous effect in a p53-dependent manner (Rizzotto et al., 2021; Shieh et al., 2000). On the other hand, it has been reported that Chk1 can also inhibit cancer cell

survival in a p53-independent manner, offering a potential avenue for cancer treatment (McNeely et al., 2014). First, characteristics of the Chk1 mRNA were investigated by analyzing gene expression profiling data from CRC cases in three public datasets. Upon analysis of CRC cases from the TCGA public dataset (Cases: Tumor/Normal = 286/41), expression of Chk1 was found to be significantly higher in CRC tumors compared with expression in normal tissue (Chk1 expression: 8.7 vs. 7.6, $p < 0.01$; Fig. 4A). Another public dataset (GSE104645) included 181 CRC cases with information on achievement of complete response (CR) towards systemic chemotherapy (Cases: CR/nonCR = 8/173). Analysis of this dataset revealed that expression of Chk1 was significantly lower in cases with CR vs. those with non-CR (Chk1 expression: −0.6 vs. 0.1, $p = 0.01$; Fig. 4B). Furthermore, analysis of the GSE159216 dataset which included survival information of stage IV CRC cases (Cases: Chk1 expression high/low = 152/19) revealed significantly poor overall survival (OS) in Chk1-high expression cases vs. Chk1-low expression cases ($p < 0.01$; Fig. 4C).

After evaluating the impact of Chk1 in CRC patients, we performed qRT-PCR assays for Chk1 and TP53 genes to identify the roles of these genes as potential culprits for orchestrating the anti-cancer effects of ABE. In fact, we observed that ABE significantly downregulated the expression of Chk1 in both SW480 (Control vs. ABE IC_{25} vs. ABE IC_{50}, 1.00 vs. 0.14 vs. 0.04; $p < 0.05 – 0.01$) and HCT116 (Control vs. ABE IC_{25} vs. ABE IC_{50}, 1.00 vs. 0.32 vs. 0.16; $p < 0.01 – 0.001$) in a dose-dependent manner (Fig. 4D). Likewise, while we did not observe a significant change in HCT116 cells, the expression of TP53 gene was also downregulated in SW480 after treatment with ABE (Control vs. ABE IC_{25} vs. ABE IC_{50}, 1.00 vs. 0.23 vs. 0.03; $p < 0.01 – 0.001$; Fig. 4D).

The phosphorylated forms of Chk1 and p53, phospho-Chk1 (p-Chk1), and phospho-p53 (p-p53) were also included in our Chk1 and p53 protein expression analysis. After normalizing with β-Actin, p-Chk1 was revealed to be significantly downregulated by ABE in both SW480 (Relative p-Chk1 expression: Control vs. ABE IC_{25} vs. ABE IC_{50}, 1.00 vs. 0.57 vs. 0.36; $p < 0.001 – 0.01$) and HCT116 (Control vs. ABE IC_{25} vs. ABE IC_{50}, 1.00 vs. 0.39 vs. 0.10; $p < 0.001$) dose-dependently (Fig. 4E). Expression of p-p53 was also downregulated in a dose-dependent manner in HCT116 after treatment with ABE (Control vs. ABE IC_{25} vs. ABE IC_{50}, 1.00 vs. 0.23 vs. 0.13; $p < 0.001$). ABE at IC_{50} concentrations downregulated p-p53 expression significantly in SW480 cells (Control vs. ABE IC_{50}, 1.00 vs. 0.62; $p < 0.01 – 0.001$; Fig. 4E). Taken together, ABE downregulated Chk1 in CRC cells, which is a prominent candidate gene for systemic therapy in CRC. Furthermore, ABE downregulated p-Chk1 and p-p53 expression, partly explaining the anti-cancer mechanism of ABE in this malignancy.

ABE caused cell cycle arrest and enhanced DNA damage in CRC cells.

Given the role of Chk1 and p53 as potential mediators of ABE's anti-cancer efficacy, we next performed cell cycle assays to examine the effect of ABE on any cell cycle dynamics. It was intriguing to observe that we observed an increase in the proportion of cells arrested in the G2/M phase following treatment with ABE at the IC_{50} concentrations in both SW480 ($p < 0.01$) and HCT116 ($p < 0.05$) cells, indicating that one of the mechanisms of its anti-cancer efficacy is through the induction of cell cycle arrest in CRC cells (Fig. 5A).

In the next step, we analyzed the expression of phosphorylated-H2A histone family member X (p-H2AX) to analyze the DNA damage in CRC cells (Fujii, 2019; Hopp et al., 2017; Takahashi et al., 2011). First, we analyzed p-H2AX expression by performing a flow cytometry assay using the Muse Cell Analyzer. For SW480, p-H2AX expression was significantly enhanced after ABE treatment with both doses of IC_{25} and IC_{50} (p-H2AX (%): Control vs. ABE IC_{25} vs. ABE IC_{50}, 20 vs. 34 vs. 36; $p < 0.05$). Similarly, ABE at IC_{50} concentration significantly enhanced p-H2AX expression in HCT116 cells (p-H2AX (%): Control vs. ABE IC_{50}, 22 vs. 34; $p < 0.05$; Fig. 5B). The results of these two p-H2HX analyses suggest that DNA damage in CRC cells was enhanced by treatment with ABE. Simultaneously, we performed immunofluorescence analysis to visualize the upregulated p-H2AX in nuclear cells responding to DNA damage (Bhardwaj et al., 2012; Mah et al., 2010)Immunofluorescence analysis for p-H2AX revealed weak expression of p-H2AX in the nontreatment control group and enhanced expression of p-H2AX in the nuclear CRC cells after ABE treatment (Fig. 5C). Collectively, our data demonstrate that ABE induces cell cycle arrest and enhances DNA damage of CRC cells.

Treatment with ABE exerted anti-cancer activity in CRC patient-derived 3D organoid (PDO) models.

The anti-cancer effects of ABE were also evaluated in PDO models previously generated from CRC cases to validate our cell culture-based findings (Okuno et al., 2022). In PDO #1, the formation of PDOs was significantly inhibited with ABE treatment with a dose of IC25 and IC50 (Number of PDOs: Control vs. ABE IC_{25} vs. ABE IC_{50}, 107 vs. 70 vs. 41; $p < 0.01 – 0.001$; Fig. 6A). In PDO #2, the PDO formation was significantly inhibited with ABE treatment at the IC_{50} concentrations (Number of PDOs: Control vs. ABE IC_{25} vs. ABE IC_{50}, 43 vs. 31 vs. 21; $p < 0.01 – 0.001$; Fig. 6A). Similarly, PDO growth was significantly inhibited in PDO #1 and #2 with ABE treatment with a dose of IC_{25} and IC_{50} (%Size of PDO#1: Control vs. ABE IC_{25} vs. ABE IC_{50}, 1.0 vs. 0.66 vs. 0.53, $p < 0.01 – 0.001$; %Size of PDO#2: Control vs. ABE IC_{25} vs. ABE IC_{50}, 1.0 vs. 0.66 vs. 0.44, $p < 0.01 – 0.001$; Fig. 6A). Overall, ABE exerted anti-cancer activity in PDOs, successfully validating our cell culture-based findings in 3D culture experiments.

DISCUSSION

The recent development of anti-cancer agents has significantly improved the survival outcomes in patients with CRC (Van Cutsem et al., 2016); however, most patients often develop chemoresistance to conventional therapeutic regimens and experience unreasonable toxicity, highlighting the need for further development of anti-cancer agents to improve treatment outcomes and quality of life. Owing to their cost-effectiveness, reduced toxicity, and ability to target multiple pathways, natural dietary compounds are increasingly considered promising complementary and alternative therapies in various cancers (Goel and Aggarwal, 2010; Goel et al., 2008a; Goel et al., 2008b; Pan et al., 2015; Wang et al., 2011; Wang et al., 2013). In this regard, we focused on ABE, which is rich in polyphenols and has a strong anti-cancer effect. In the present study, we performed a series of comprehensive and systematic studies in CRC cell lines with diverse genomic backgrounds. Subsequently, we validated these findings in PDOs to evaluate the anti-cancer effect and mechanisms of ABE.

The anti-cancer effects of ABE on cell viability have been previously reported in a few recent studies in pancreatic cancer (Thani et al., 2014), hepatocellular carcinoma (Gao et al., 2018), leukemia (Sharif et al., 2012), cervical cancer (Rugina et al., 2012), and CRC (Bermudez-Soto et al., 2007; Malik et al., 2003; Zhao et al., 2004). However, most of these studies were primarily exploratory and did not delve deeper into the specific mechanism(s) of ABE's anti-cancer activity. Our present study demonstrates that ABE inhibited cell viability, migration, clonogenicity, and invasion in CRC cell lines. More importantly, previous studies suggested that excessive ROS accumulation in cancer cells can lead to cell death, including apoptosis (Wang et al., 2021). In the present study, we demonstrate the efficacy of ABE in enhancing ROS accumulation and inducing apoptosis in CRC cells, which is in line with some of the suggestions made in previous reports (Rugina et al., 2012; Wei et al., 2020). The paradoxical effect of antioxidants on ROS accumulation and cancer cell death has often been reported in previous studies (Kalyanaraman et al., 2018; Xu et al., 2023). This effect partly explains the accumulation of ROS and the subsequent cell death induced by ABE in the present study. Genome-wide transcriptomic analysis, first performed in our study in CRC cells, allowed us to identify key growth signaling pathways associated with ABE's anti-cancer activity, including the p53 signaling pathway. While previous reports have not focused on the effect of ABE on specific genes related to the p53 signaling pathway, we validated key differentially regulated genes within the p53 signaling cascade using qRT-PCR assays (Fig. 6B).

After confirming the p53 signaling pathway as one of the top 10 enriched KEGG pathways, we examined the role of Chk1 as a key regulator of p53 (Hu et al., 2021) and its candidacy as a target in anti-cancer therapy (da Costa et al., 2023). Chk1 is a Ser/Thr protein kinase that causes the Intra-S and G2/M phase cell cycle arrest (Neizer-Ashun and Bhattacharya, 2021) and is activated through phosphorylation, responding to DNA damage (Han et al., 2016). Chk1 is capable of controlling the cell cycle dynamics through the regulation of p53 activity and inhibiting the phosphorylation of cyclin-dependent kinases (CDKs), which are the key regulators of the cell cycle (McNeely et al., 2014). From the analysis of the TCGA dataset, we found that overexpression of Chk1 has been reported in various malignancies, including CRC (Madoz-Gurpide et al., 2007). Furthermore, our additional assessments of Chk1 in the public datasets GSE104645 and GSE159216 confirmed that Chk1 promotes tumor growth in CRC and several malignancies, thus highlighting a relationship between Chk1, resistance to anti-cancer agents (Bartucci et al., 2012; Cavelier et al., 2009; Lee et al., 2011; Perego et al., 2003) and tumor progression. The present study suggested that p-Chk1 was downregulated with p-p53 by ABE in both CRC cell lines, SW480 with mutated p53 mutation and HCT116 with wild type p53, resulting in cell cycle arrest in G2/M phase and enhancement of DNA damage evaluated with p-H2AX expression.

There are several strengths to our study. First, we conducted a genome-wide transcriptomic analysis to investigate the anti-cancer effects of ABE in CRC cells and to identify the specific genes and pathways involved in its anti-cancer efficacy. As a result of these efforts, we observed a significant enrichment of various pathways, particularly the p53 signaling pathway. Further analysis of key regulators within the p53 signaling pathway revealed that both Chk1 and p53 were downregulated by ABE, which enhanced DNA damage. Second, we employed two different treatment concentrations (IC_{25} and IC_{50}) to confirm their anti-

cancer efficacy. Third, the anti-cancer efficacy of ABE was successfully validated in the PDO model.

We would like to acknowledge some of the limitations of the present study. First, the effect of ABE was not evaluated in an animal model. Second, we did not directly assess the potential toxicity of ABE in normal cells; however, previous studies have reported that ABE did not have any adverse effects on nontumorigenic colon cells when used at such low concentrations (Zhao et al., 2004), and there are no reports of severe adverse effects after evaluating the impact of ABE on small animal models (Gajić et al., 2020) or clinical patients (Kędzierska et al., 2013). Additionally, our study did not include a positive control drug, which might have allowed for comparisons between ABE and clinically utilized drugs. Furthermore, this study evaluated ABE solely as a monotherapy, even though polyphenols have demonstrated enhanced antitumor effects when combined with existing systemic therapies (Kaviani et al., 2023). Future research must determine its compatibility and potential synergistic effects with current therapeutic regimens.

In conclusion, these findings provide additional evidence for using ABE as a safe, cost-effective, and multi-targeted complementary and integrative therapeutic modality in colorectal cancer. The potential of ABE in preventing and treating colorectal cancer, including its use in combination with existing systemic therapies, requires further investigation.

Supplementary Material

Refer to Web version on PubMed Central for supplementary material.

ACKNOWLEDGEMENTS

The authors thank Yuan Li, Katsuki Miyazaki, Silei Sui, Courtney Quan, Tikam Dakal, Qinghua Huang, Souvick Roy, Nour-Lynn Mouallem, and Bianca Hua for their thoughtful discussions and advice during this project.

Funding:

This work was supported by CA184792, CA187956, CA227602, CA072851, and CA202797 grants from the National Cancer Institute National Institutes of Health.

Abbreviations:

ABE	Aronia berry extract
ATCC	American type culture collection
Chk1	Checkpoint kinase 1
CRC	Colorectal cancer
DNA	Deoxyribonucleic acid
DMEM	Dulbecco’s Modified Eagle’s medium
DMSO	Dimethyl sulfoxide

FBS	Fetal bovine serum
OD	Optical density
GO	Gene ontology
KEGG	Kyoto Encyclopedia of Genes and Genomes
PBS	Phosphate-buffered saline
PDO	Patient-derived organoids
ROS	Reactive oxygen species
qRT-PCT	Quantitative reverse transcription polymerase chain reaction

REFERENCES

1. Bartucci M, Svensson S, Romania P, Dattilo R, Patrizii M, Signore M, Navarra S, Lotti F, Biffoni M, Pilozzi E, Duranti E, Martinelli S, Rinaldo C, Zeuner A, Maugeri-Sacca M, Eramo A, De Maria R, 2012. Therapeutic targeting of Chk1 in NSCLC stem cells during chemotherapy. Cell Death Differ 19, 768–778. [PubMed: 22117197]
2. Bermudez-Soto MJ, Larrosa M, Garcia-Cantalejo JM, Espin JC, Tomas-Barberan FA, Garcia-Conesa MT, 2007. Up-regulation of tumor suppressor carcinoembryonic antigen-related cell adhesion molecule 1 in human colon cancer Caco-2 cells following repetitive exposure to dietary levels of a polyphenol-rich chokeberry juice. J Nutr Biochem 18, 259–271. [PubMed: 16860979]
3. Bhardwaj V, Zhan Y, Cortez MA, Ang KK, Molkentine D, Munshi A, Raju U, Komaki R, Heymach JV, Welsh J, 2012. C-Met inhibitor MK-8003 radiosensitizes c-Met-expressing non-small-cell lung cancer cells with radiation-induced c-Met-expression. J Thorac Oncol 7, 1211–1217. [PubMed: 22617250]
4. Bouyahya A, Omari NE, El Hachlafi N, Jemly ME, Hakkour M, Balahbib A, El Menyiy N, Bakrim S, Naceiri Mrabti H, Khouchlaa A, Mahomoodally MF, Catauro M, Montesano D, Zengin G, 2022. Chemical Compounds of Berry-Derived Polyphenols and Their Effects on Gut Microbiota, Inflammation, and Cancer. Molecules 27, 1–59.
5. Cavelier C, Didier C, Prade N, Mansat-De Mas V, Manenti S, Recher C, Demur C, Ducommun B, 2009. Constitutive activation of the DNA damage signaling pathway in acute myeloid leukemia with complex karyotype: potential importance for checkpoint targeting therapy. Cancer Res 69, 8652–8661. [PubMed: 19843865]
6. da Costa A, Chowdhury D, Shapiro GI, D'Andrea AD, Konstantinopoulos PA, 2023. Targeting replication stress in cancer therapy. Nat Rev Drug Discov 22, 38–58. [PubMed: 36202931]
7. Del Rio D, Borges G, Crozier A, 2010. Berry flavonoids and phenolics: bioavailability and evidence of protective effects. Br J Nutr 104 Suppl 3, S67–90. [PubMed: 20955651]
8. Fujii Y, 2019. DNA Damage Focus Formation Assay. Methods Mol Biol 1984, 69–73. [PubMed: 31267421]
9. Gajić D, Saksida T, Koprivica I, Šenerović L, Morić I, Šavikin K, Menković N, Pejnović N, Stojanović I, 2020. Immunomodulatory activity and protective effects of chokeberry fruit extract on Listeria monocytogenes infection in mice. Food Funct. 11, 9, 7793–7803. [PubMed: 32808624]
10. Gao N, Wang Y, Jiao X, Chou S, Li E, Li B, 2018. Preparative Purification of Polyphenols from Aronia melanocarpa (Chokeberry) with Cellular Antioxidant and Antiproliferative Activity. Molecules 23, 1–14.
11. Goel A, Aggarwal BB, 2010. Curcumin, the golden spice from Indian saffron, is a chemosensitizer and radiosensitizer for tumors and chemoprotector and radioprotector for normal organs. Nutr Cancer 62, 919–930. [PubMed: 20924967]
12. Goel A, Jhurani S, Aggarwal BB, 2008a. Multi-targeted therapy by curcumin: how spicy is it? Mol Nutr Food Res 52, 1010–1030. [PubMed: 18384098]

13. Goel A, Kunnumakkara AB, Aggarwal BB, 2008b. Curcumin as “Curecumin”: from kitchen to clinic. Biochem Pharmacol 75, 787–809. [PubMed: 17900536]
14. Han X, Tang J, Wang J, Ren F, Zheng J, Gragg M, Kiser P, Park PS, Palczewski K, Yao X, Zhang Y, 2016. Conformational Change of Human Checkpoint Kinase 1 (Chk1) Induced by DNA Damage. J Biol Chem 291, 12951–12959. [PubMed: 27129240]
15. Hernandez Borrero LJ, El-Deiry WS, 2021. Tumor suppressor p53: Biology, signaling pathways, and therapeutic targeting. Biochim Biophys Acta Rev Cancer 1876, 1–32.
16. Hopp N, Hagen J, Aggeler B, Kalyuzhny AE, 2017. Express gamma-H2AX Immunocytochemical Detection of DNA Damage. Methods Mol Biol 1644, 123–128.
17. Hu J, Cao J, Topatana W, Juengpanich S, Li S, Zhang B, Shen J, Cai L, Cai X, Chen M, 2021. Targeting mutant p53 for cancer therapy: direct and indirect strategies. J Hematol Oncol 14, 157, 1-19. [PubMed: 34583722]
18. Kalyanaraman B, Cheng G, Hardy M, Ouari O, Bennett B, Zielonka J., 2018. Teaching the basics of reactive oxygen species and their relevance to cancer biology: Mitochondrial reactive oxygen species detection, redox signaling, and targeted therapies. Redox Biol 15, 347–362. [PubMed: 29306792]
19. Kaviani E, Hajibabaie F, Abedpoor N, Safavi K, Ahmadi Z, Karimy A, 2023. System biology analysis to develop diagnostic biomarkers, monitoring pathological indexes, and novel therapeutic approaches for immune targeting based on maggot bioactive compounds and polyphenolic cocktails in mice with gastric cancer. Environ Res 238, 117168. [PubMed: 37742751]
20. Gajić D, Saksida T, Koprivica I, Šenerović L, Morić I, Šavikin K, Menković N, Pejnović N, Stojanović I, 2020. Immunomodulatory activity and protective effects of chokeberry fruit extract on Listeria monocytogenes infection in mice. Food Funct. 11, 9, 7793–7803. [PubMed: 32808624]
21. Lee JH, Choy ML, Ngo L, Venta-Perez G, Marks PA, 2011. Role of checkpoint kinase 1 (Chk1) in the mechanisms of resistance to histone deacetylase inhibitors. Proc Natl Acad Sci U S A 108, 19629–19634. [PubMed: 22106282]
22. Madoz-Gurpide J, Canamero M, Sanchez L, Solano J, Alfonso P, Casal JI, 2007. A proteomics analysis of cell signaling alterations in colorectal cancer. Mol Cell Proteomics 6, 2150–2164. [PubMed: 17848589]
23. Mah LJ, El-Osta A, Karagiannis TC, 2010. gammaH2AX: a sensitive molecular marker of DNA damage and repair. Leukemia 24, 679–686. [PubMed: 20130602]
24. Malik M, Zhao C, Schoene N, Guisti MM, Moyer MP, Magnuson BA, 2003. Anthocyanin-rich extract from Aronia meloncarpa E induces a cell cycle block in colon cancer but not normal colonic cells. Nutr Cancer 46, 186–196. [PubMed: 14690795]
25. McNeely S, Beckmann R, Bence Lin AK, 2014. CHEK again: revisiting the development of CHK1 inhibitors for cancer therapy. Pharmacol Ther 142, 1–10. [PubMed: 24140082]
26. Neizer-Ashun F, Bhattacharya R, 2021. Reality CHEK: Understanding the biology and clinical potential of CHK1. Cancer Lett 497, 202–211. [PubMed: 32991949]
27. Okuno K, Garg R, Yuan YC, Tokunaga M, Kinugasa Y, Goel A, 2022. Berberine and Oligomeric Proanthocyanidins Exhibit Synergistic Efficacy Through Regulation of PI3K-Akt Signaling Pathway in Colorectal Cancer. Front Oncol 12, 855–860.
28. Pan P, Skaer CW, Stirdivant SM, Young MR, Stoner GD, Lechner JF, Huang YW, Wang LS, 2015. Beneficial Regulation of Metabolic Profiles by Black Raspberries in Human Colorectal Cancer Patients. Cancer Prev Res (Phila) 8, 743–750. [PubMed: 26054356]
29. Perego P, Gatti L, Righetti SC, Beretta GL, Carenini N, Corna E, Dal Bo L, Tinelli S, Colangelo D, Leone R, Apostoli P, Lombardi L, Beggiolin G, Piazzoni L, Zunino F, 2003. Development of resistance to a trinuclear platinum complex in ovarian carcinoma cells. Int J Cancer 105, 617–624. [PubMed: 12740909]
30. Ravindranathan P, Pasham D, Balaji U, Cardenas J, Gu J, Toden S, Goel A, 2018. A combination of curcumin and oligomeric proanthocyanidins offer superior anti-tumorigenic properties in colorectal cancer. Sci Rep 8, 1–12. [PubMed: 29311619]
31. Rizzotto D, Englmaier L, Villunger A, 2021. At a Crossroads to Cancer: How p53-Induced Cell Fate Decisions Secure Genome Integrity. Int J Mol Sci 22, 1–19.

32. Roy S, Zhao Y, Yuan YC, Goel A, 2022. Metformin and ICG-001 Act Synergistically to Abrogate Cancer Stem Cells-Mediated Chemoresistance in Colorectal Cancer by Promoting Apoptosis and Autophagy. Cancers (Basel) 14, 1–19.
33. Rugina D, Sconta Z, Leopold L, Pintea A, Bunea A, Socaciu C, 2012. Antioxidant activities of chokeberry extracts and the cytotoxic action of their anthocyanin fraction on HeLa human cervical tumor cells. J Med Food 15, 700–706. [PubMed: 22846076]
34. Sharif T, Alhosin M, Auger C, Minker C, Kim JH, Etienne-Selloum N, Bories P, Gronemeyer H, Lobstein A, Bronner C, Fuhrmann G, Schini-Kerth VB, 2012. Aronia melanocarpa juice induces a redox-sensitive p73-related caspase 3-dependent apoptosis in human leukemia cells. PLoS One 7, 1–11.
35. Sharma P, Shimura T, Banwait JK, Goel A, 2020. Andrographis-mediated chemosensitization through activation of ferroptosis and suppression of β-catenin/Wnt-signaling pathways in colorectal cancer. Carcinogenesis 41, 1385–1394. [PubMed: 32835374]
36. Shieh SY, Ahn J, Tamai K, Taya Y, Prives C, 2000. The human homologs of checkpoint kinases Chk1 and Cds1 (Chk2) phosphorylate p53 at multiple DNA damage-inducible sites. Genes Dev 14, 289–300. [PubMed: 10673501]
37. Siegel RL, Miller KD, Fuchs HE, Jemal A, 2021. Cancer Statistics, 2021. CA Cancer J Clin 71, 7–33. [PubMed: 33433946]
38. Sung H, Ferlay J, Siegel RL, Laversanne M, Soerjomataram I, Jemal A, Bray F, 2021. Global Cancer Statistics 2020: GLOBOCAN Estimates of Incidence and Mortality Worldwide for 36 Cancers in 185 Countries. CA Cancer J Clin 71, 209–249. [PubMed: 33538338]
39. Takahashi M, Koi M, Balaguer F, Boland CR, Goel A, 2011. MSH3 mediates sensitization of colorectal cancer cells to cisplatin, oxaliplatin, and a poly(ADP-ribose) polymerase inhibitor. J Biol Chem 286, 12157–12165. [PubMed: 21285347]
40. Thani NA, Keshavarz S, Lwaleed BA, Cooper AJ, Rooprai HK, 2014. Cytotoxicity of gemcitabine enhanced by polyphenolics from Aronia melanocarpa in pancreatic cancer cell line AsPC-1. J Clin Pathol 67, 949–954. [PubMed: 25232128]
41. Van Cutsem E, Cervantes A, Adam R, Sobrero A, Van Krieken JH, Aderka D, Aranda Aguilar E, Bardelli A, Benson A, Bodoky G, Ciardiello F, D'Hoore A, Diaz-Rubio E, Douillard JY, Ducreux M, Falcone A, Grothey A, Gruenberger T, Haustermans K, Heinemann V, Hoff P, Kohne CH, Labianca R, Laurent-Puig P, Ma B, Maughan T, Muro K, Normanno N, Osterlund P, Oyen WJ, Papamichael D, Pentheroudakis G, Pfeiffer P, Price TJ, Punt C, Ricke J, Roth A, Salazar R, Scheithauer W, Schmoll HJ, Tabernero J, Taieb J, Tejpar S, Wasan H, Yoshino T, Zaanan A, Arnold D, 2016. ESMO consensus guidelines for the management of patients with metastatic colorectal cancer. Ann Oncol 27, 1386–1422. [PubMed: 27380959]
42. Wang LS, Arnold M, Huang YW, Sardo C, Seguin C, Martin E, Huang TH, Riedl K, Schwartz S, Frankel W, Pearl D, Xu Y, Winston J 3rd, Yang GY, Stoner G, 2011. Modulation of genetic and epigenetic biomarkers of colorectal cancer in humans by black raspberries: a phase I pilot study. Clin Cancer Res 17, 598–610. [PubMed: 21123457]
43. Wang LS, Kuo CT, Cho SJ, Seguin C, Siddiqui J, Stoner K, Weng YI, Huang TH, Tichelaar J, Yearsley M, Stoner GD, Huang YW, 2013. Black raspberry-derived anthocyanins demethylate tumor suppressor genes through the inhibition of DNMT1 and DNMT3B in colon cancer cells. Nutr Cancer 65, 118–125. [PubMed: 23368921]
44. Wang Y, Qi H, Liu Y, Duan C, Liu X, Xia T, Chen D, Piao HL, Liu HX, 2021. The double-edged roles of ROS in cancer prevention and therapy. Theranostics 11, 4839–4857. [PubMed: 33754031]
45. Wei J, Yu W, Hao R, Fan J, Gao J, 2020. Anthocyanins from Aronia melanocarpa Induce Apoptosis in Caco-2 Cells through Wnt/beta-Catenin Signaling Pathway. Chem Biodivers 17, 1–11.
46. Xu C, Wang M, Zandieh Doulabi B, Sun Y, Liu Y., 2023. Paradox: Curcumin, a Natural Antioxidant, Suppresses Osteosarcoma Cells via Excessive Reactive Oxygen Species. Int J Mol Sci 24, 15, 11975.
47. Zhao C, Giusti MM, Malik M, Moyer MP, Magnuson BA, 2004. Effects of commercial anthocyanin-rich extracts on colonic cancer and nontumorigenic colonic cell growth. J Agric Food Chem 52, 6122–6128. [PubMed: 15453676]

48. Zhao Y, Roy S, Wang C, Goel A, 2022a. A Combined Treatment with Berberine and Andrographis Exhibits Enhanced Anti-Cancer Activity through Suppression of DNA Replication in Colorectal Cancer. Pharmaceuticals (Basel) 15, 1–17.

49. Zhao Y, Wang C, Goel A, 2022. A combined treatment with melatonin and andrographis promotes autophagy and anticancer activity in colorectal cancer. Carcinogenesis 43, 217–230. [PubMed: 35089340]

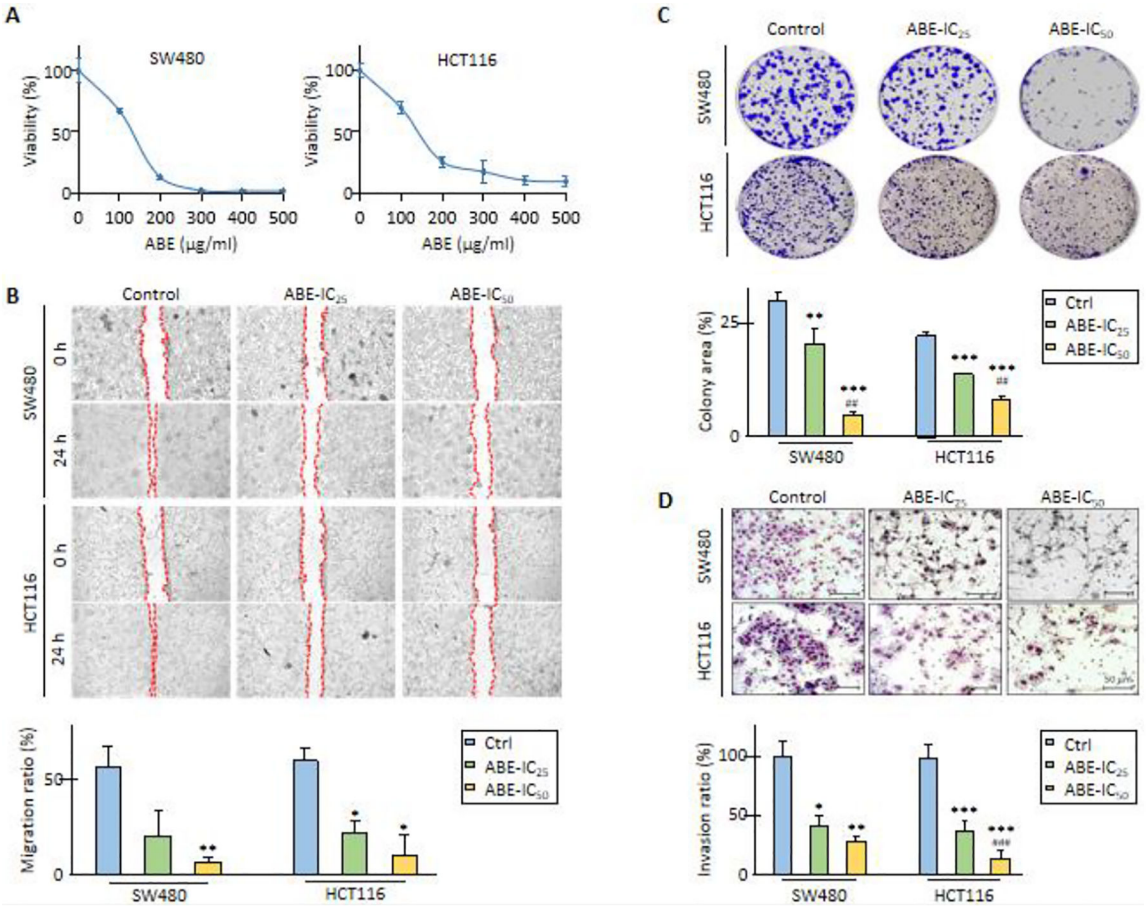

Figure 1:

Anti-cancer effects of ABE in CRC cells. **(A)** The line graphs depict the results of the MTT assays for cell viability in SW480 and HCT116 cell lines following treatment with different concentrations of ABE for 48 hours. ABE suppressed the cell viability in both CRC cells in a dose-dependent manner. **(B)** Migration assay after treatment with ABE for 24 hours. ABE treatment at IC_{50} concentrations inhibited cell migration in both CRC cell lines. **(C)** Colony formation assay after treatment with ABE. ABE treatment using IC_{25} and IC_{50} concentrations significantly inhibited clonogenicity in both CRC cell lines in a dose-dependent manner. **(D)** Invasion assay using CRC cells after treatment with ABE for 48 hours. ABE treatment using IC_{25} and IC_{50} doses inhibited the invasive ability in both CRC cell lines. Moreover, the anti-invasive effects of ABE were dose-dependent in HCT116 cells. Error bars are the mean ± SD. (*; *P* value < 0.05 vs. control, **; *P* value < 0.01 vs. control, ***; *P* value < 0.001 vs. control, $^{\#\#}$; *P* value < 0.01 vs. ABE-IC_{25}, $^{\#\#\#}$; *P* value < 0.001 vs. ABE-IC_{25}). ABE, Aronia berry extract; CRC, colorectal cancer.

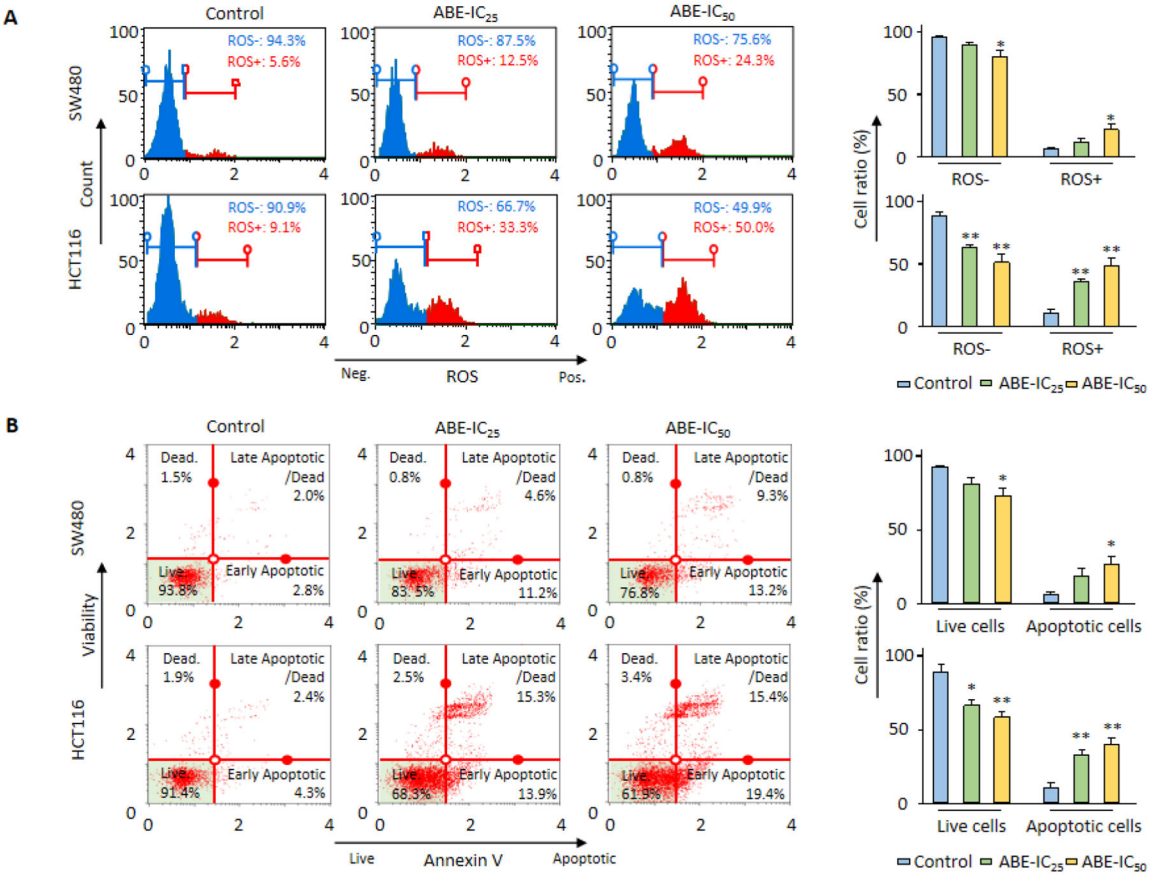

Figure 2:

ABE induces ROS accumulation and enhances apoptosis in CRC cells. **(A)** Representative histograms for the ROS distribution in SW480 and HCT116 cells after treatment with ABE for 24 hours. Values are expressed as the percentage of ROS- (negative) and ROS+ (positive) cells in the bar graphs. ABE concentrations at IC_{50} levels induced ROS accumulation in SW480 cells, and IC_{25} concentrations and higher doses induced ROS accumulation in HCT116 cells. **(B)** Representative histograms for the cells undergoing apoptosis in Annexin V binding assay in SW480 and HCT116 cell lines after treatment with ABE for 24 hours. Values are expressed as the percentage of alive and apoptotic cells, which is the total of early and late apoptotic cells, in the bar graphs. ABE enhanced apoptosis at IC_{50} concentrations in SW480 cells and IC_{25} concentrations in HCT116 cells. (*; *P* value < 0.05 vs. control, **; *P* value < 0.01 vs. control). ABE, Aronia berry extract; CRC, colorectal cancer; ROS, reactive oxygen species.

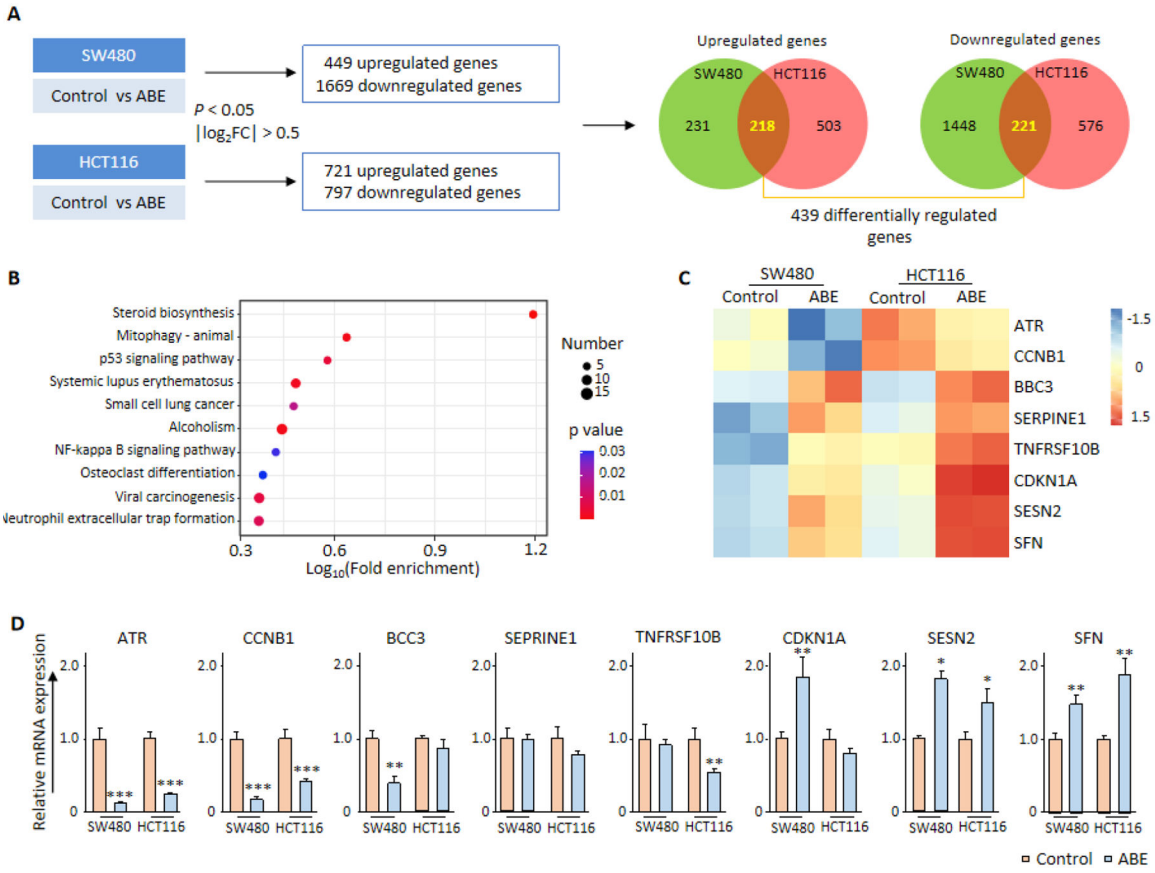

Figure 3:

P53 signaling pathway correlates with anti-carcinogenic effects of ABE in CRC cells. **(A)** Schema showing the procedure for selecting differentially regulated genes according to the genome-wide transcriptomic analysis of CRC cells in the ABE treatment group and control group. A gene was defined as up- or down-regulated when it had the Log_2 FC > ±0.5 and $P < 0.05$ difference between ABE treatment and control in SW480 or HCT116 cells. Four hundred thirty-nine genes up- or down-regulated in both cell lines were defined as common differentially regulated genes between the two cell lines. **(B)** Scatter plots of KEGG pathway enrichment analysis of common differentially regulated genes in ABE-treated CRC cells. A pathway was considered enriched with a fold enrichment > 2.0 and $P < 0.05$ with gene number > 5. The top 10 enriched pathways are plotted in the figure. **(C)** Heatmap illustrating the expression of common differentially regulated genes in the p53 signaling pathway. (D) qRT-PCR analysis of common differentially regulated genes within the p53 signaling pathway in SW480 and HCT116 cells. β-Actin mRNA expression was used for an internal control. The average (column) ± SD is indicated (*; *P* value < 0.05, **; *P* value < 0.01, ***; *P* value < 0.001 control vs. ABE). ABE, Aronia berry extract; CRC, colorectal cancer; KEGG, Kyoto Encyclopedia of Genes and Genomes.

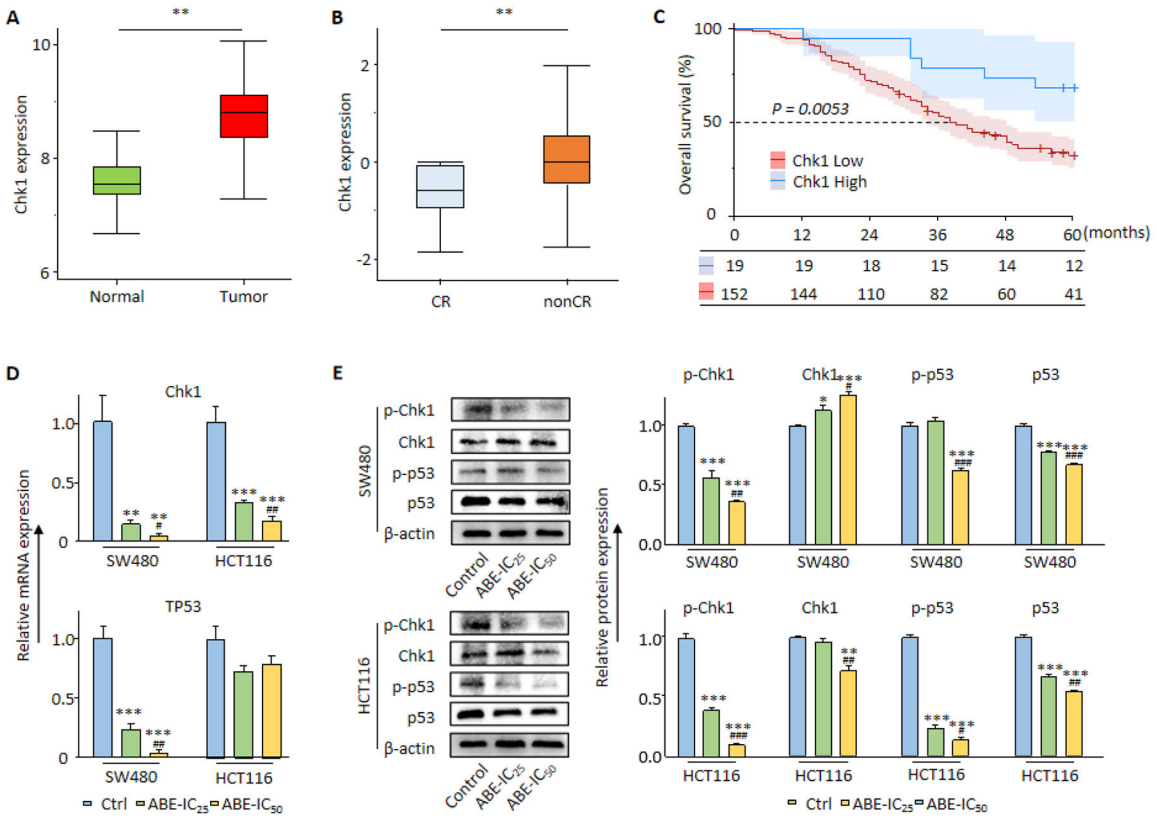

Figure 4:

ABE inhibits Chk1 expression in CRC cells, a potential target for systemic therapy in CRC. **(A)** Expression of Chk1 in CRC cases from the TCGA dataset. Expression of Chk1 was upregulated in tumors vs. normal tissues. **(B)** Expression of Chk1 in CRC cases from GSE104645. Expression of Chk1 was high in nonCR (complete response) cases compared to those with CR cases after systemic therapy in CRC. **(C)** Expression of Chk1 in CRC cases from GSE GSE159216. Stage IV CRC with high Chk1 expression was associated with poor survival outcomes. **(D)** qRT-PCR analyses of Chk1 and TP53 in SW480 and HCT116 cells after treatment with different concentrations of ABE for 24 hours. β-actin mRNA expression was used as an internal control to calculate the relative expression of genes. **(E)** Western immunoblotting of p53 signaling pathway-related proteins (ATR, p-ATR, ATM, p-ATM, p53, and p-p53) and β-actin in SW480 and HCT116 cells after treatment with different concentrations of ABE for 24 hours. β-actin protein was used for internal control. The average (column) ± SD is indicated (*; *P* value < 0.05 vs. control, **; *P* value < 0.01 vs. control, ***; *P* value < 0.001 vs. control, #; *P* value < 0.05 vs. ABE-IC_{25}, ##; *P* value < 0.01 vs. ABE-IC_{25}, ###; *P* value < 0.001 vs. ABE-IC_{25}). ABE, Aronia berry extract; Chk1, Checkpoint kinase 1; CR, complete response.

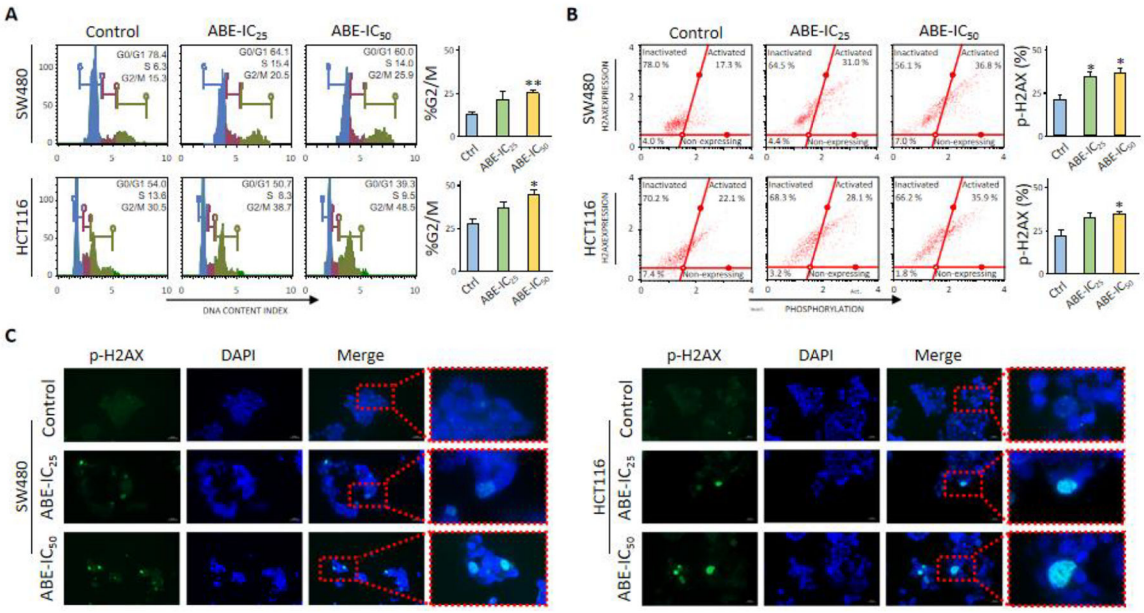

Figure 5:

ABE-caused cell cycle arrest in the G2/M phase and enhanced DNA damage in CRC cells. **(A)** Representative histograms illustrating cell cycle arrest in the G2/M phase for both cell lines following ABE treatment. **(B)** Representative histograms for the p-H2AX representing DNA damage in SW480 and HCT116 cells after treatment with different concentrations of ABE for 48 hours. Values are expressed as the percentage of p-H2AX expressed cells. **(C)** Representative images for immunofluorescence assay for p-H2AX with its expression enhanced in nuclear for both CRC cells after treatment with ABE. The average (column) ± SD is indicated (*; *P* value < 0.05 vs. control, **; *P* value < 0.01 vs. control). ABE, Aronia berry extract; H2AX, H2A histone family member X, p-; phosphorylated-.

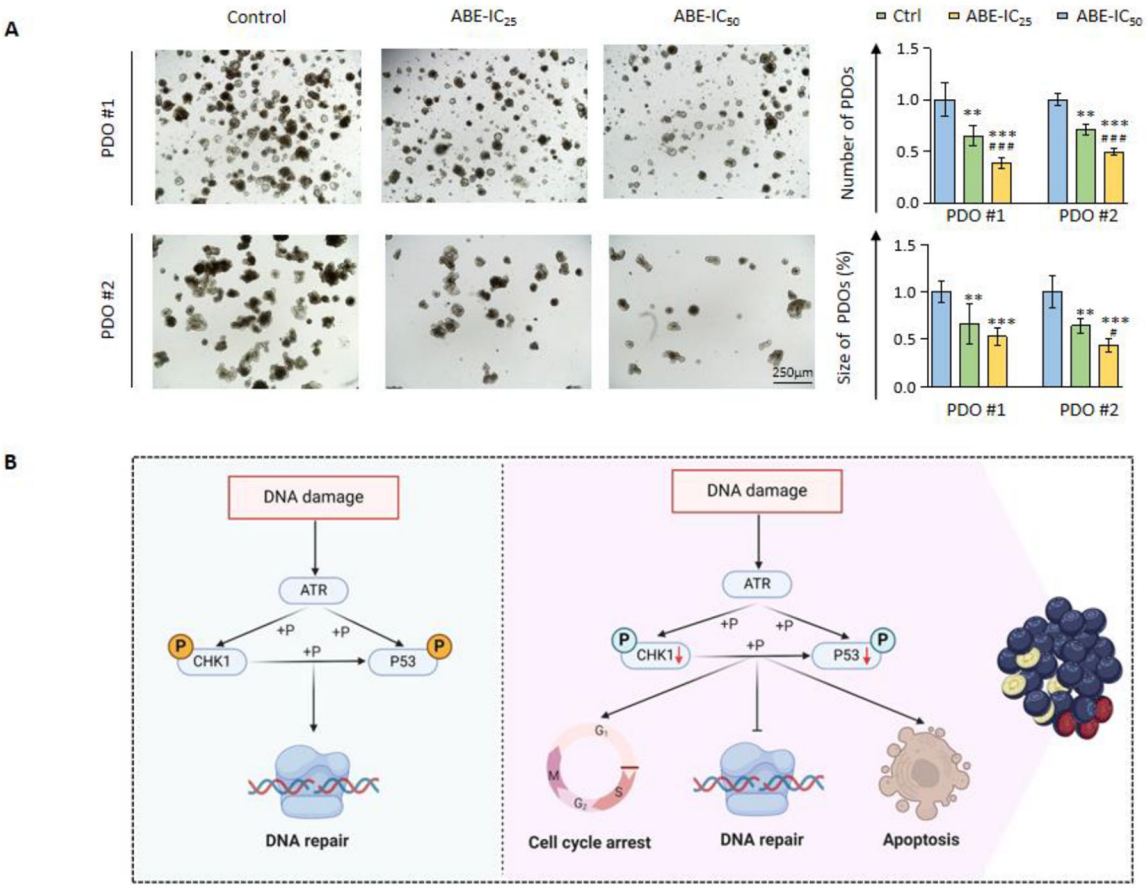

Figure 6:

ABE effectively enhanced anti-cancer activity in CRC patient-derived 3D organoid (PDO) models and a graphical abstract illustrating the effect of ABE on CRC cells. **(A)** Representative images of PDOs following treatment with different concentrations of ABE for 48 hours. The average (column) ± SD of PDO counts and size are indicated (*; *P* value < 0.05 vs. control, **; *P* value < 0.01 vs. control, ***; *P* value < 0.001 vs. control). B) A schematic illustration of the anti-cancer effect of ABE through the regulation of DNA damage by Chk1 and p53 in CRC. **(B)** A schematic illustration depicting the effect of ABE on CRC cells. ABE, Aronia berry extract; Chk1, Checkpoint kinase 1; PDO, patient-derived 3D organoid.